On the molecular theory of aqueous electrolyte solutions. II. Structural and thermodynamic properties of different models at infinite dilution

P. G. Kusalik[a] and G. N. Patey
Department of Chemistry, University of British Columbia, Vancouver, British Columbia, Canada V6T 1Y6

This paper describes a comparative theoretical study of the infinite dilution properties of solutions of univalent ions in different water-like solvents. The theoretical results are obtained by solving the reference hypernetted-chain (RHNC) approximation as described in the first article of this series [J. Chem. Phys. **88**, 7715 (1988)]. It is shown that the inclusion of the octupole moment of the water molecule in the model solvent leads to strong preferential solvation of negative ions, and that this has important effects upon certain thermodynamic properties and upon the ion–solvent and ion–ion structure. Questions concerning the definition and physical interpretation of individual ion partial molar volumes are raised and considered in detail. It is argued that in general the individual ion results obtained experimentally may not accurately reflect the true microscopic ion–solvent structure.

I. INTRODUCTION

In paper I (Ref. 1) of this series we have described a theoretical study of model aqueous electrolytes at finite ion concentration. The model considered consisted of hard sphere ions immersed in a polarizable dipole tetrahedral–quadrupole solvent (referred to below as model I). The calculations were carried out by solving the reference hypernetted-chain (RHNC) equations with solvent polarization effects treated at the self-consistent mean field (SCMF) level.[2] The principal purpose of the present article is to investigate the influence of varying the water-like solvent model upon the thermodynamic and structural properties at infinite dilution. Particular attention is paid to the definition and calculation of the partial molar volumes of individual ions. It is argued that even at infinite dilution these single-ion quantities are not uniquely defined and great care should be taken in their physical interpretation.

Calculations were carried out for a variety of univalent ions immersed in three model water-like solvents which for convenience we shall refer to as models I, II, and III. All three models are hard spheres of the same diameter, and all three include the polarizability tensor α and the dipole moment μ. The models differ at the quadrupole and octupole levels and can be summarized as follows:

Model I: $(\alpha, \mu, \text{tetrahedral-}\mathbf{Q},)$

Model II: $(\alpha, \mu, \mathbf{Q})$,

Model III: $(\alpha, \mu, \mathbf{Q}, \boldsymbol{\Omega})$,

where the parameters enclosed in brackets are those included in the calculation of the electrostatic interactions. The expression "tetrahedral-Q" refers to the approximate quadrupole moment defined by Eq. (32) of Ref. 1, and $\mathbf{Q}$ and $\boldsymbol{\Omega}$ are the correct quadrupole and octupole moments, respectively, of the water molecule.

The general equations describing the various pair interactions (i.e., ion–ion, ion–solvent, and solvent–solvent) for the present models are given in Ref. 1. This is also true of the SCMF/RHNC equations and of the method of numerical solution. Hence in the present paper it is usually sufficient to ignore the theoretical details and focus upon the results obtained. An exception to this occurs in Sec. II B, where certain interesting theoretical questions concerning the definition of single-ion partial molar volumes are discussed in some detail.

II. RESULTS AND DISCUSSION

For models I and II the molecular parameters used in the present calculations are those summarized in Table I of Ref. 1. For the water molecule the octupole tensor is completely defined by specifying the elements Ω_{xxz}, Ω_{yyz}, and Ω_{zzz} which must obey the condition $\Omega_{xxz} + \Omega_{yyz} + \Omega_{zzz} = 0$. For model III the values[3] 2.30×10^{-34}, -0.96×10^{-34}, and -1.34×10^{-34} esu cm^3 were used for Ω_{xxz}, Ω_{yyz}, and Ω_{zzz}, respectively. A detailed account of the SCMF/RHNC results for models I–III will be given elsewhere.[4] The values of the pure solvent dielectric constant ϵ_0 and of the mean and effective dipole moments

TABLE I. Values of the mean dipole moment m', the effective dipole moment m_e, and the dielectric constant ϵ_0, given by the SCMF/RHNC theory (Ref. 4) for the different model solvents. The dipole moments are given in Debyes.

Property	Models I and II	Model III
m'	2.584 D	2.601 D
m_e	2.632 D	2.649 D
ϵ_0	93.5	87.1

[a] Present address: Research School of Chemistry, Australian National University, Canberra, Australian Capital Territory 2601, Australia.

(m' and m_e, respectively) obtained for models II and III at 25 °C are given in Table I. We recall that the value of the tetrahedral–quadrupole moment used in model I was adjusted such as to give essentially the same bulk properties as model II. It can be seen from Table I that at least some of the properties of the pure solvent are not very sensitive to the presence of the octupole moment. The value of ϵ_0 is reduced a little but is still considerably larger than the experimental result (i.e., 78.5).

The reduced ion diameters defined by $d_i^* = d_i/d_s$, where d_i and d_s are the ion and solvent hard sphere diameters, used in our calculations are included in Table II below. The origin of these values is discussed in Ref. 1 and here we simply recall that d_s is taken to be 2.8 Å. In addition to the alkali metal and halide ions we also consider the fictitious ions M^+, Eq^+, and Eq^-. As in Ref. 1, M^+ is used as a model for large cations such as $(C_2H_5)_4NH_3^+$. The ions Eq^+ and Eq^- are of equal diameter (i.e., $d_+ = d_- = d_s$) and hence they help to clearly reveal the asymmetric solvation of cations and anions immersed in solvents II and III.

It was found that the differences in the thermodynamic and structural properties obtained for models I and II were small in comparison with those observed for models I and III. Hence only the solvent I and III results are explicitly compared in the following discussion.

A. Ion–solvent energies and structure

The average ion–solvent energies (obtained in the effective system[1]) per ion for models I and III are compared in Table II. We note that although the average ion–octupole energy is rather small (i.e.,$\leqslant 5\%$ of U_{is}), the total octupole induced change in U_{is} is ~10%– 11% for the smaller ions. Also, the asymmetric nature of the solvation is apparent if we consider pairs of positive and negative ions of equal size (e.g., Na^+/F^-, Eq^+/Eq^-, and Cs^+/Br^-). It is clear that for model III the solvent interacts more strongly with the anion than with the cation. For example, the total ion–solvent interaction energy for Na^+ is about 20% more positive than the total interaction with F^-. It should be noted that the energies given in Table II cannot be compared with experimental hydration energies[5] since the experimental results contain a solvent–solvent contribution[6] in addition to the ion–solvent term calculated here.

The ion–solvent radial distribution functions $g_{is}(r)$ for Na^+ and F^- are plotted in Fig. 1. Results for models I and III are included, and we recall that for model I, $g_{is}(r)$ is equivalent for Na^+ and F^-. It can be seen that when the octupole is added the contract peak increases substantially for F^- and decreases for Na^+. This reflects the preferential solvation of negative ions discussed above. The influence of the octupole can also be seen in the second peak where the Na^+ curve again decreases in height. For larger ions (e.g., Cs^+, Br^-) similar effects are observed in comparing $g_{is}(r)$ for models I and III. However, the changes induced by the octupole moment are less pronounced which is as we would expect in view of the fact that the ion–octupole interaction decreases as r_{is}^{-4}.

Coordination numbers (CN) estimated using the formula

$$CN = 4\pi\rho_s \int_0^R r^2 g_{is}(r)\,dr, \qquad (1)$$

TABLE II. Average ion–solvent energies and coordination numbers (CN) for models I and III. U_{iD}, U_{iQ}, U_{iO}, and U_{is} are the ion–dipole, ion–quadrupole, ion–octupole, and total ion–solvent interactions, respectively. The numbers in brackets are the reduced ion diameters d_i^*.

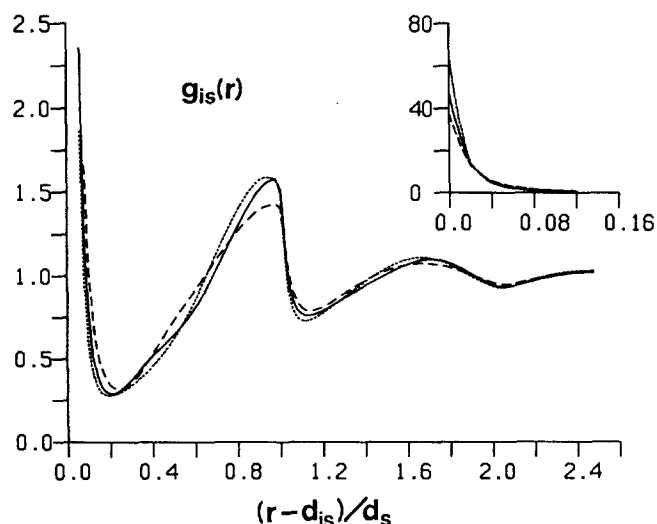| Ion	Solvent	$\beta U_{iD}/N_i$	$\beta U_{iQ}/N_i$	$\beta U_{iO}/N_i$	$\beta U_{is}/N_i$	CN
Li$^+$ (0.68)	I	−394.0	−62.7		−456.7	8.74
	III	−372.9	−49.5	11.2	−411.2	8.12
Na$^+$ (0.84)	I	−331.6	−46.6		−378.1	8.00
	III	−320.9	−37.1	6.5	−351.4	7.64
Eq$^+$ (1.0)	I	−287.0	−36.1		−323.0	7.65
	III	−282.2	−29.1	3.7	−307.5	7.44
K$^+$ (1.08)	I	−269.5	−31.7		−301.2	7.57
	III	−266.5	−26.0	2.8	−289.7	7.41
Cs$^+$ (1.28)	I	−234.5	−23.7		−258.2	7.79
	III	−234.6	−20.3	1.3	−253.6	7.46
M$^+$ (1.96)	I	−165.1	−10.6		−175.7	9.79
	III	−169.6	−11.0	−0.3	−180.9	8.54
F$^-$ (0.84)	I	−331.6	−46.6		−378.1	8.00
	III	−337.1	−63.0	−22.2	−422.2	8.90
Eq$^-$ (1.0)	I	−287.0	−36.1		−323.0	7.65
	III	−293.3	−43.2	−12.7	−349.1	8.24
Cl$^-$ (1.16)	I	−254.2	−28.1		−282.3	7.53
	III	−259.2	−30.8	−7.6	−297.6	7.91
Br$^-$ (1.28)	I	−234.5	−23.7		−258.2	7.79
	III	−238.4	−24.4	−5.3	−268.2	7.81
I$^-$ (1.44)	I	−212.9	−19.2		−232.1	8.00
	III	−215.3	−18.3	−3.3	−236.9	8.11

FIG. 1. Ion–solvent radial distribution functions. The solid curve represents the results for Na^+ or F^- in model I. The dashed and dotted curves are for Na^+ and F^-, respectively, in model III.

where R is the value of r at which $g_{is}(r)$ reaches its first minimum, are included in Table II. We observe that the influence of the octupole on the coordination numbers is as would be anticipated from the $g_{is}(r)$ curves discussed above. For positive ions the CN is decreased by the octupolar interactions and for negative ions it is increased. For model III the CN of Na$^+$ is lower than that of Cl$^-$ whereas the opposite is true for model I. The model III results are in better accord with computer simulation studies[7–11] of these ions in different water-like models.

The orientational structure of solvent molecules in the vicinity of an ion can be examined by plotting the function $\langle \cos \theta_{is}(r) \rangle$ as defined by Eqs. (60) of Ref. 1. It is useful to recall that $\cos \theta_{+s} = \hat{\mu} \cdot \hat{r}_{+s}$ and $\cos \theta_{-s} = -(\hat{\mu} \cdot \hat{r}_{-s})$ (where $\hat{\mu}$ is a unit vector along the dipole and $\hat{r}_{is} = \mathbf{r}_{is}/|\mathbf{r}_{is}|$) and hence $\cos \theta_{is}$ is positive for attractive dipolar orientations for both positive and negative ions. The curves obtained for Na$^+$ and F$^-$ in solvents I and III are shown in Fig. 2. We note that for both ions the contact values decrease (i.e., the dipolar interactions are less favored) when the octupole is included, but that the effect is larger for F$^-$. In order to get an idea of the average orientation of the solvent molecules in the vicinity of an ion we average $\langle \cos \theta_{is}(r) \rangle$ over the first solvation shell to obtain $\langle \cos \theta_{is} \rangle_{FS}$. The "average" angle is then estimated by supposing that $\langle \theta_{is} \rangle_{FS} \simeq \cos^{-1}(\langle \cos \theta_{is} \rangle_{FS})$. For Na$^+$ and F$^-$ in solvent III we find 54.5° and 56.4°, respectively, compared with the value 52.7° obtained for both ions in model I. Thus, in the first shell, the average orientation of the dipole vector does not change greatly and for both solvent models $\langle \theta_{is} \rangle_{FS}$ is close to one-half of the tetrahedral angle (i.e., 54.5°). For the other positive and negative ions considered the variation of $\langle \cos \theta_{is}(r) \rangle$ with solvent model is qualitatively similar to that shown in Fig. 2. In both solvents the values of $\langle \theta_{is} \rangle_{FS}$ increase a little with ion size. For example, in solvent III we obtain 56.5°, 58.3°, 57.8°, and 59.4° for K$^+$, Cs$^+$, Cl$^-$, and Br$^-$, respectively.
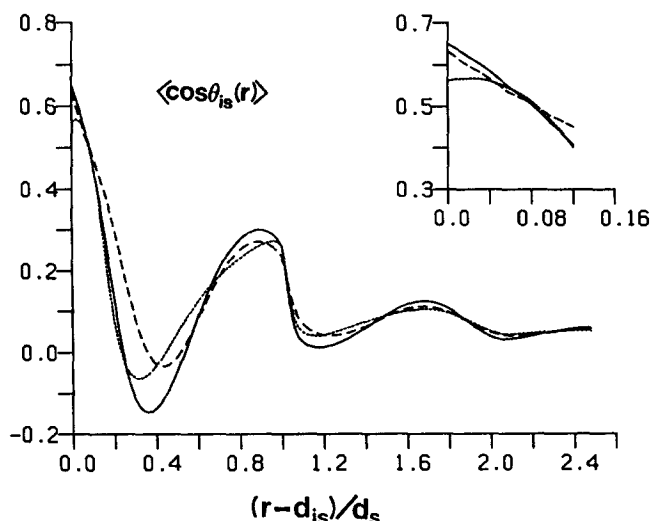
B. Partial molar volumes

In this section we consider the partial molar volumes at infinite dilution of the various salts, and of the individual ions. The partial molar volumes of the individual ions are of particular interest since these quantities are sometimes used[5,12] to infer information about the ion–solvent interactions. It is argued below that this procedure may be fraught with previously unsuspected pitfalls since the partial molar volumes of *individual ions* obtained experimentally may not reflect the true ion–solvent correlation and interaction at infinite dilution.

In the following we shall closely follow the methods and notation of Refs. 13 and 1, and usually we shall simply refer to equations given in the earlier articles. However, it is useful to recall here the key definitions:

$$G_{\alpha\beta} = \tilde{h}^{000}_{00;\alpha\beta}(0) = 4\pi \int r^2 h^{000}_{00;\alpha\beta}(r)dr, \qquad (2)$$

$$C_{\alpha\beta} = \tilde{c}^{000}_{00;\alpha\beta}(0) = 4\pi \int r^2 c^{000}_{00;\alpha\beta}(r)dr, \qquad (3)$$

where $\tilde{h}^{000}_{00;\alpha\beta}(k)$ and $\tilde{c}^{000}_{00;\alpha\beta}(k)$ are the Fourier transforms of the radial pair and direct correlation functions, respectively [cf. Eq. (6b) of Ref. 13]. In Ref. 13 it is shown that at infinite dilution the partial molecular volume of the solute (i.e., salt) in a general M$_{\nu_+}$X$_{\nu_-}$/solvent system is given by

$$\overline{V}^0_2 = \nu_+ k_B T \chi^0_T (1 - \rho_s C^0_{+s})$$
$$+ \nu_- k_B T \chi^0_T (1 - \rho_s C^0_{-s}), \qquad (4)$$

where ρ_s is the solvent density, $k_B T$ is the Boltzmann constant times the absolute temperature, and χ^0_T is the isothermal compressibility of the pure solvent.

In Table III infinite dilution values for the partial molar volumes of LiF, NaCl, KBr, and CsI in models I and III are compared with experimental results[14] for aqueous electrolytes at 25 °C. From Eq. (4) it can be seen that $\overline{V}^0_2$ is proportional to the isothermal compressibility of the solvent. In our previous article[1] is was pointed out that the present model solvents (at least when treated at the RHNC level) are several times more compressible than real water. Thus in Table III we have also included the theoretical values for $\overline{V}^0_2$ obtained using the experimental result for χ^0_T in Eq. (4). Examination of the results given in Table III indicates that the theoretical values are all in poor quantitative agreement with experiment, although the theoretical calculations do give the

FIG. 2. The function $\langle \cos \theta_{is}(r) \rangle$ for Na$^+$ and F$^-$. The curves are as in Fig. 1.

TABLE III. Theoretical and experimental results for the partial molar volumes at infinite dilution of several alkali halide salts. The experimental values were constructed from the single ion partial molar volumes given in Ref. 14. The theoretical numbers enclosed in parentheses were obtained by using the experimental value for χ^0_T in Eq. (4). All results are in units of cm^3 mol^{-1}.

Salt	Model I		Model III		Experimental
LiF	− 118.6 (− 32.0)		− 146.3 (− 30.2)		− 2.04
NaCl	− 36.3 (− 9.8)		− 48.9 (− 10.1)		16.6
KBr	19.6 (5.3)		15.3 (3.1)		33.7
CsI	74.4 (20.1)		80.4 (16.6)		57.6

correct qualitative dependence upon ion size. The inclusion of the octupole moment in the solvent model does not improve the theoretical estimates of $\bar{V}_2^0$. It is likely that the large discrepancies between theory and experiment for $\bar{V}_2^0$ reflect the fact that the hard sphere potential must provide only a very crude approximation to the short-range ion–solvent and solvent–solvent interactions.

The partial molar volume of a salt is a well defined quantity which extrapolates smoothly (following a square root law) to its limiting value $\bar{V}_2^0$ at infinite dilution. However, what exactly is meant by the partial molar volume of an *individual ion* is not so well defined. The experimental values reported for these quantities are usually obtained by rather arbitrarily splitting the $\bar{V}_2^0$ results into component parts based upon a variety of physical assumptions concerning the partial molar volumes of certain ions (c.f. a number of methods are summarized in Refs. 14 and 15). One experimental technique which does give absolute values for the partial molar volumes of individual ions is that based upon ultrasonic vibration potentials,[15,16] and this method is briefly discussed below. Our purpose here is to attempt to define individual ion partial molar volumes from a theoretical perspective and, particularly, to explore the relationship between these quantities and the ion–solvent interactions.

Within the framework of Kirkwood–Buff theory[17] as applied to electrolytes in Ref. 13 at least two microscopic expressions for individual ion partial molar volumes at infinite dilution appear possible. One expression can be obtained by simply comparing the definition (again assuming a salt of the type $M_{\nu_+} X_{\nu_-}$)

$$\bar{V}_2 = \nu_+ \bar{V}_+ + \nu_- \bar{V}_- \qquad (5)$$

with Eq. (4). This immediately yields

$$\bar{V}_i^{0*} = k_B T \chi_T^0 \left(1 - \rho_s C_{is}^0 \right), \qquad (6)$$

where C_{is}^0 is given by Eq. (3) and the asterisk is used to simply indicate an individual ion partial molar volume as defined by Eq. (6). It is argued below that the individual ion values extracted from experimental measurements are likely closely related to $\bar{V}_i^{0*}$.

Another approach is to define $\bar{V}_i^0$ as the volume change which results when a *single* ion i is added to an infinite (i.e., without boundaries) bath containing only pure solvent. Obviously, this is not an experiment which could be carried out in practice, but it is nevertheless an appropriate definition of an individual ion partial molar volume at infinite dilution. Furthermore, it is this single-ion picture which one has in mind when one attempts to physically interpret the individual ion quantities.

For this two species single-ion/solvent system in the $\rho_i = 0$ limit the appropriate Kirkwood–Buff expressions[13,17] immediately yield the result

$$\bar{V}_i^0 = \frac{1}{\rho_s} + G_{ss}^0 - G_{is}^0 = k_B T \chi_T^0 - G_{is}^0, \qquad (7)$$

where the final form follows from the well-known relationship (cf. Ref. 13 and references therein)

$$1 + \rho_s G_{ss}^0 = (1 - \rho_s C_{ss}^0)^{-1} = \rho_s k_B T \chi_T^0. \qquad (8)$$

Our next task is to determine how $\bar{V}_i^0$ is related to the $\bar{V}_i^{0*}$ defined above.

In order to do this we recall[1] that in the limit $\rho_+ = \rho_- = 0$, the Ornstein–Zernike equation leads to the exact relationship

$$\tilde{h}_{00;is}^{000}(k) - \tilde{c}_{00;is}^{000}(k)$$

$$= \rho_s \sum_m Z_m \sum_{\omega = -m}^{m} (-)^{\omega} \tilde{h}_{0\omega;is}^{0mm}(k) \, \tilde{c}_{-\omega 0;ss}^{m0m}(k), \qquad (9)$$

where Z_m is a known nonzero constant dependent only on m, and $\tilde{h}_{0\omega;is}^{0mm}(k)$ and $\tilde{c}_{-\omega 0;ss}^{m0m}(k)$ are Hankel transforms of the r-dependent coefficients in the rotational invariant expansions of the correlation functions as defined in earlier articles.[1,18,19] In order to take the $k \to 0$ limit of Eq. (9) we need simply note that in the vicinity of $k = 0$ (cf. Refs. 20 and 21)

$$\tilde{h}_{0\omega;is}^{011}(k) = -i \left(\tilde{h}_{0\omega;is}^{011(-1)} k^{-1} + \tilde{h}_{0\omega;is}^{011(1)} k + \cdots \right) \qquad (10)$$

and

$$\tilde{c}_{-\omega 0;ss}^{101}(k) = -i\tilde{c}_{-\omega 0;ss}^{101(1)} k + \dots \, . \qquad (11)$$

These expansions together with the observations[1,13,20,21] that for $m > 1$, $\tilde{h}_{0\omega;is}^{0mm}(0) \to$ a constant if $m = 2$ [due to the charge–quadrupole interaction, $h_{0\omega;is}^{022}(r)$ decays as r^{-3} as $r \to \infty$] or zero if $m > 2$ [the $h_{0\omega;is}^{0mm}(r)$ fall faster than r^{-3}], and that $\tilde{c}_{\omega 0;ss}^{m0m}(0) = 0$ for $m > 0$ (since the solvent is uncharged the $c_{-\omega 0;ss}^{m0m}(r)$ all decay faster than r^{-3}) allow us to immediately write

$$G_{is}^0 = \frac{C_{is}^0}{1 - \rho_s C_{ss}^0} - \frac{\rho_s Z_1}{1 - \rho_s C_{ss}^0}$$

$$\times \sum_{\omega = -1}^{1} (-)^{\omega} \tilde{h}_{0\omega;is}^{011(-1)} \tilde{c}_{-\omega 0;ss}^{101(1)}, \qquad (12)$$

which is a general exact result at $k = 0$.

We remark that the expressions given for G_{is}^0 in Ref. 13 [cf. Eqs. (40a) and (40b)] include only the first term in Eq. (12) and hence do not hold in general. In fact Eqs. (40a) and (40b) of Ref. 13 are simplified relationships valid for solvents which satisfy certain symmetry requirements. In particular, the last term in Eq. (12) obviously vanishes if $(mnl) \equiv (101)$ is not allowed in the solvent–solvent correlation functions. This is true for purely dipolar particles and for solvent model I considered in the present paper and in Ref. 1.

However, for models II and III terms with $(mnl) \equiv (101)$ are allowed in the solvent–solvent correlation functions and the second term in Eq. (12) will contribute to G_{is}^0. Furthermore, since these models are of C_{2v} symmetry only the lower index $\omega = 0$ will occur and it is convenient to rewrite Eq. (12) in the form

$$G_{is}^0 = \rho_s k_B T \chi_T^0 \left(C_{is}^0 + T_{is}^0 \right), \qquad (13)$$

where

$$T_{is}^0 = -\rho_s Z_1 \tilde{h}_{00;is}^{011(-1)} \tilde{c}_{00;ss}^{101(1)}, \qquad (14)$$

and we have used Eq. (8). Also for this case the exact form of $\tilde{h}_{00;is}^{011(-1)}$ can be derived from the known[22] long-range behavior of $h_{00;ss}^{011}(r)$ and T_{is}^0 can be written explicitly as

$$T_{is}^0 = -\frac{4\pi\beta q_i m_e}{9y} \left(\frac{\epsilon_0 - 1}{\epsilon_0}\right) \frac{4\pi}{3} \rho_s \int r^3 c_{00;ss}^{101}(r) dr, \tag{15}$$

where ϵ_0 is the dielectric constant of the pure solvent, q_i is the ionic charge, $y = 4\pi\beta m_e^2 \rho_s/9$, $\beta = 1/k_B T$, and in determining Z_1 we have taken the rotational invariants to be defined by Eqs. (5) and (36) of Ref. 19. It is clear that T_{is}^0 depends only upon the ionic charge and pure solvent properties, and that, furthermore, for ions of equal but opposite charge $T_{+s}^0 = -T_{-s}^0$. We emphasize that T_{is}^0 is not in any sense a continuum contribution. It is in fact a *model dependent* term which arises from the coupling between ion–solvent and solvent–solvent orientational correlations.

Returning now to $\overline{V}_i^0$ and substituting Eq. (13) into Eq. (7) we obtain

$$\overline{V}_i^0 = k_B T \chi_T^0 (1 - \rho_s C_{is}^0 - \rho_s T_{is}^0), \tag{16}$$

which is the desired result. Comparing Eqs. (6) and (16) we see that $\overline{V}_i^0 = \overline{V}_i^{0*}$ only for models for which $T_{is}^0 = 0$. At this point in our discussion two remarks are worthwhile. First, due to the fact that T_{is}^0 is proportional to q_i the T_{+s}^0 and T_{-s}^0 contributions to $\overline{V}_2^0$ will always *cancel exactly*. Thus for the partial molar volume of the salt Eq. (4) is always recovered regardless as to whether $\overline{V}_i^0$ or $\overline{V}_i^{0*}$ is taken to be the definition of the single-ion quantities. Second, it should be emphasized that the existence of T_{is}^0 depends upon the fact that we are considering the unscreened case of a single ion in a solvent bath. At all finite concentrations screening ensures that $\tilde{h}_{00;is}^{011}(k) = 0$ at $k = 0$ and T_{is} vanishes. We shall see below that comparing $\overline{V}_i^0$ and $\overline{V}_i^{0*}$ is very instructive when we attempt to understand the relationship between individual ion partial molar volumes and the ion–solvent energies and structure.

Before discussing the numerical results for the single-ion quantities it is useful to consider the different experimental situations in a little more detail. As mentioned earlier experimental estimates of absolute individual ion partial molar volumes have been obtained[14] using a number of different assumptions. Clearly, since the values found depend upon the underlying assumption all results reported cannot be described by a single microscopic formula. However, as noted above, the T_{is}^0 terms do not contribute to $\overline{V}_2^0$ and, furthermore, these terms do not appear to have been taken into account in any of the assumptions made in order to separate $\overline{V}_2^0$ into individual ion contributions. Therefore, it seems

reasonable to suppose that (insofar as they are described by any microscopic expression at all) the individual ion results obtained by dividing the $\overline{V}_2^0$ values must correspond to $\overline{V}_i^{0*}$. The ultrasonic vibration potential method which directly produces absolute values for the individual ion quantities deserves closer attention.

Debye[16] first predicted in 1933 that ultrasonic waves when applied to an electrolyte solution would generate an alternating electrical potential which should be measureable. However, it has been only relatively recently[15] that this technique has been used to determine individual ion partial molar volumes. Very briefly, the phenomenon itself results[16] from the fact that in solution the "effective masses" of the hydrated ions will not be the same, and hence the response of the cations and anions to the applied ultrasonic signal will be different. Consequently, local regions of higher cation and anion concentrations will develop and these give rise to measureable potential differences. The potential difference is related to the differences in molar masses, which in turn can be related to differences in the partial molar volumes of individual ions.[15] Knowledge of $\overline{V}_2$ then allows the determination of individual ion quantities and infinite dilution results are obtained by extrapolation. Our purpose here is to make a *suggestion* as to what the finite concentration individual ion "partial molar volumes" measured by this method might be in terms of the various correlation functions, and to see what is obtained when such results are extrapolated to infinite dilution.

From the above discussion it is clear that the experimental technique relies upon a local "disruption" of charge neutrality in order to determine individual ion quantities. In Ref. 13 we have shown that k-dependent analogs of the Kirkwood–Buff equations can be used to obtain exact determinate expressions for certain thermodynamic properties of electrolyte solutions (including $\overline{V}_2$) by taking the appropriate $k \to 0$ limit analytically. Now in the formulation given in Ref. 13 the condition $k \to 0$ simply represents the local charge neutrality limit, and the finite k quantities can in a sense be regarded as describing a situation where local neutrality has been disturbed, e.g., by an ultrasonic wave. Thus it seems reasonable to suggest that the individual ion partial molar volumes obtained using the ultrasonic method might correspond microscopically to the appropriate k-dependent Kirkwood–Buff expression evaluated at some small but nonzero k. We emphasize that this assertion is speculative, but it is interesting in any case to look at the $k \to 0$ followed by the $\rho_2 \to 0$ limit (note that the order in which the limits are taken is important here) of the k-dependent individual ion quantities.

Taking the k-dependent partial molecular volume of species i, $\widetilde{V}_i(k)$, to be defined by Eq. (12b) of Ref. 13, and carrying out some manipulation along the lines followed in our earlier work,[13] we find that as $k \to 0$,

$$\widetilde{V}_i(k) \to \frac{\rho_i \rho_j^2 \rho_s^2 k^2 \{[1/\rho_s + \tilde{h}_{ss}^{(0)}][\tilde{h}_{jj}^{(2)} - \tilde{h}_{ij}^{(2)}] + \tilde{h}_{is}^{(0)}[\tilde{h}_{is}^{(2)} - \tilde{h}_{js}^{(2)} + \tilde{h}_{ij}^{(2)} - \tilde{h}_{ji}^{(2)}] + \tilde{h}_{ij}^{(0)}[\tilde{h}_{js}^{(2)} - \tilde{h}_{is}^{(2)}]\}}{\rho_i^2 \rho_j^2 \rho_s^2 k^2 \{[1/\rho_s + \tilde{h}_{ss}^{(0)} + \tilde{h}_{ij}^{(0)} - 2\tilde{h}_{is}^{(0)}][\tilde{h}_{ii}^{(2)} + \tilde{h}_{jj}^{(2)} - 2\tilde{h}_{ij}^{(2)}]\}}, \tag{17}$$

where we have used the notation of Ref. 13. Equation (17) is valid at finite concentrations and $\tilde{V}_i(k)$ is well defined and independent of k in the small k limit. Also it can be seen that $\widetilde{\widetilde{V}}_i(0)$ has (not unexpectedly) a rather complicated dependence upon the zeroth and second moments of the radial correlation functions between *all* species in solution. The zeroth moment $\tilde{h}_{\alpha\beta}^{(0)} \equiv G_{\alpha\beta}^0$ [cf. Eq. (2)], and the second moments are given by[13,21]

$$\tilde{h}_{\alpha\beta}^{(2)} = -\frac{4\pi}{6} \int r^4 h_{00;\alpha\beta}^{000}(r)dr. \tag{18}$$

We are interested in the $\rho_2 \to 0$ limit of Eq. (17), and in order to take this limit it is necessary to know the limiting behavior of the zeroth and second moments. The limiting expressions for the zeroth moments were previously derived [cf. Eqs. (33), (39), and (44) of Ref. 13]. The required limits of the second moments can be obtained by inserting the low concentration large separation limiting forms of the various $h_{00;\alpha\beta}^{000}(r)$ [cf. Eqs. (B6), (B7), and (B9) of Ref. 1] into Eq. (18) and carrying out the necessary integrations. Retaining only the leading terms in ρ_2 we obtain that as $\rho_2 \to 0$,

$$\tilde{h}_{ii}^{(2)} \to \frac{\epsilon_0 k_B T}{4\pi q_j^2 v^2 \rho_2^2}, \tag{19}$$

$$\tilde{h}_{ij}^{(2)} \to \frac{\epsilon_0 k_B T}{4\pi q_i q_j v^2 \rho_2^2}, \tag{20}$$

$$\tilde{h}_{is}^{(2)} \to \frac{\rho_s (k_B T)^2 \chi_T^0 \epsilon_0 q_i}{4\pi (q_i q_j)^2 v^2 \rho_2} (C_{is} v_i q_i + C_{js} v_j q_j), \tag{21}$$

and

$$\tilde{h}_{ss}^{(2)} \to \frac{\rho_s^2 (k_B T)^3 (\chi_T^0)^2 \epsilon_0}{4\pi (q_i q_j)^2 v^2} (C_{is} v_i q_i + C_{js} v_j q_j)^2, \tag{22}$$

where $v = v_+ + v_-$. Then making the necessary substitutions into Eq. (17) and simplifying we obtain the final result

$$\widetilde{\widetilde{V}}_i(0) \to k_B T \chi_T^0 (1 - \rho_s C_{is}^0) \tag{23}$$

as $\rho_2 \to 0$. The right-hand side of Eq. (23) is clearly just the quantity $\overline{V}_i^{0*}$ defined by Eq. (6). This analysis supports the conjecture that the experimentally determined individual ion partial molar volumes at infinite dilution can be correctly identified as $\overline{V}_i^{0*}$.

We are now ready to discuss the numerical results, and values for $\overline{V}_i^{0*}$ and $\overline{V}_i^0$ obtained using Eqs. (6) and (16), respectively, are given in Table IV. Results for both models I and III are included. We note that the experimental result for χ_T^0 has been used in these calculations in order to remove differences arising simply from the fact that the compressibilities of the respective solvents are not identical. This also gives more meaningful numbers to compare with the experimental results since discrepancies due only to compressibility differences are removed. The experimental values given in Table IV are those obtained from ultrasonic vibration potential measurements.[15] We note that the results given by this technique are generally in fair agreement with those obtained using other methods.[15]

A number of observations can be made concerning the

TABLE IV. Individual ion partial molar volumes at infinite dilution. The theoretical results were obtained from Eqs. (6) and (16) using the experimental value of χ_T^0. The experimental values are those determined from ultrasonic vibration potentials (Ref. 15). All values are in units of $cm^3 mol^{-1}$.

Ion	Model I $\overline{V}_i^{0*} = \overline{V}_i^0$	Model III $\overline{V}_i^{0*}$	$\overline{V}_i^0$	Experimental
Li^+	−20.4	−30.6	−16.1	−11.2
Na^+	−11.6	−24.0	−9.4	−7.4
Eq^+	−4.6	−18.2	−3.6	···
K^+	−1.4	−15.3	0.8	3.4
Cs^+	6.7	−8.2	6.4	15.5
M^+	39.4	21.1	35.7	···
F^-	−11.6	0.4	−14.1	3.3
Eq^-	−4.6	7.6	−7.0	···
Cl^-	1.8	13.9	−0.7	23.7
Br^-	6.7	18.5	3.9	30.2
I^-	13.4	24.8	10.2	41.4

theoretical results given in Table IV. It is useful to focus upon the pairs Na^+/F^-, Eq^+/Eq^-, and Cs^+/Br^-, which are equal in size and equal and opposite in charge. For these pairs in model I the partial molar volumes are equal due to the symmetric solvation and, moreover, as discussed above $\overline{V}_i^{0*} = \overline{V}_i^0$ since $T_{is}^0 = 0$. However, in model III the symmetry is broken and the influence of the octupole is apparent. For $\overline{V}_i^{0*}$ the octupolar interactions have a very large effect resulting in values which are more negative for cations and more positive for anions. Furthermore, it can be seen from the table that this behavior (i.e., for ions of equal size $\overline{V}_+^{0*} < \overline{V}_-^{0*}$) is qualitatively consistent with the experimental results. Hence, for ions of equal size an examination of the $\overline{V}_i^{0*}$ values for model III would lead one to conclude that the degree of electrostriction of the solvent in the vicinity of such ions is much greater for cations than for anions. The truth of this conclusion shall be examined below. Turning to the $\overline{V}_i^0$ results obtained for model III, we see that the qualitative dependence upon the sign of the ionic charge is inverted with cations giving somewhat more positive values than anions of the same size. This rather dramatic difference between $\overline{V}_i^0$ and $\overline{V}_i^{0*}$ is a consequence of the fact that the contribution $k_B T \rho_s \chi_T^0 T_{is}^0$ to $\overline{V}_i^0$ is very large (i.e., ± 14.6 cm^3 mol^{-1}) for univalent ions in solvent III. Comparing values of $\overline{V}_i^0$ obtained for models I and III we see that the influences of the octupole upon C_{is}^0 and T_{is}^0 cancel [cf. Eq. (16)] to a large extent such that the net effect upon $\overline{V}_i^0$ is relatively small.

It is very interesting to reexamine the ion–solvent structure and energies discussed above in an attempt to understand how the partial molar volumes of individual ions might be related to the ion–solvent interactions. Returning to Fig. 1 we see that in model III the ion–solvent radial correlations at short range are stronger for F^- than for Na^+ [note that the contact value $g_{is}(d_{is})$ is considerably larger for F^- than for Na^+], and that furthermore F^- has a larger coordination number than Na^+ (i.e., ~8.9 vs 7.6). Thus, for solvent III the ion–solvent radial distribution function indicates that the neighboring solvent particles are more tightly

held by F⁻ than by Na⁺, and consequently we would expect the electrostriction of the surrounding solvent to be greater for anions than for cations. From Table IV and the discussion given above we see that this observation based upon the ion–solvent structure is consistent with the $\overline{V}_i^0$ results (i.e., $\overline{V}_-^0 < \overline{V}_+^0$), but is the exact opposite of the conclusion one would reach by comparing the $\overline{V}_i^{0*}$ values for positive and negative ions of equal size (i.e., $\overline{V}_+^{0*} < \overline{V}_-^{0*}$).

One might also expect the electrostriction of the solvent to be roughly proportional to the magnitude of the average ion–solvent interaction energy. That is, the greater the magnitude of U_{is} the greater the degree of electrostriction. Examination of the average ion–solvent energies for model III (cf. Table II) shows that for ions of equal size U_{-s} is always larger in magnitude (i.e., more negative) than U_{+s}, and hence on this basis as well we would expect the electrostriction to be greater for negative ions. This is consistent with the ion–solvent structure and with the $\overline{V}_i^0$ values, but again inconsistent with the $\overline{V}_i^{0*}$ results.

From these observations we must conclude that the individual ion partial molar volumes defined by $\overline{V}_i^{0*}$ (and which we believe to be the closest theoretical definition we have of the quantities obtained experimentally) cannot, in general, be used to deduce accurate information about the nature of the microscopic ion–solvent structure. Indeed, for model III the structural inferences one would make by comparing the $\overline{V}_i^{0*}$ results for positive and negative ions are exactly the contrary of the true situation. The quantities $\overline{V}_i^0$, which do [essentially by definition, cf. Eq. (7)] accurately reflect the true short-range ion–solvent structure, contain terms (i.e., T_{is}^0) which do not influence $\overline{V}_2^0$ and hence do not contribute to the $\overline{V}_i^{0*}$. In other words, the $\overline{V}_i^{0*}$ values (and in our opinion the experimental individual ion partial molar volumes) cannot be correctly physically interpreted by thinking in terms of a *single isolated* ion interacting with the solvent. These quantities refer to a neutral solution and even if there are only two ions present the influence of the counter ion is "felt" through the cancellation of the T_{is}^0 terms.

C. Ion–ion structure

At infinite dilution it is convenient to consider the ion–ion potentials of mean force defined by

$$\beta w_{ij}(r) = -\ln g_{ij}(r), \qquad (24)$$

where $g_{ij}(r)$ is the radial distribution function. It is shown below that $w_{ij}(r)$ is rather sensitive to the model solvent, and that this is particularly true for pairs of like ions.

The potentials of mean force for the unlike pairs Li⁺/ F⁻, Na⁺/Cl⁻, and M⁺/Br⁻ are shown in Figs. 3(a)–3(c). It is evident that for the relatively small ions Li⁺/F⁻ $\beta w_{ij}(r)$ is quite strongly influenced by the presence of the octupole. Specifically, the first maximum is considerably reduced in magnitude and the entire function is generally shifted to more negative values. For Na⁺/Cl⁻ similar effects are found but the octupole driven variations are much smaller in magnitude. For M⁺/Br⁻ the situation is essentially inverted with the curve for model III now lying above the result for
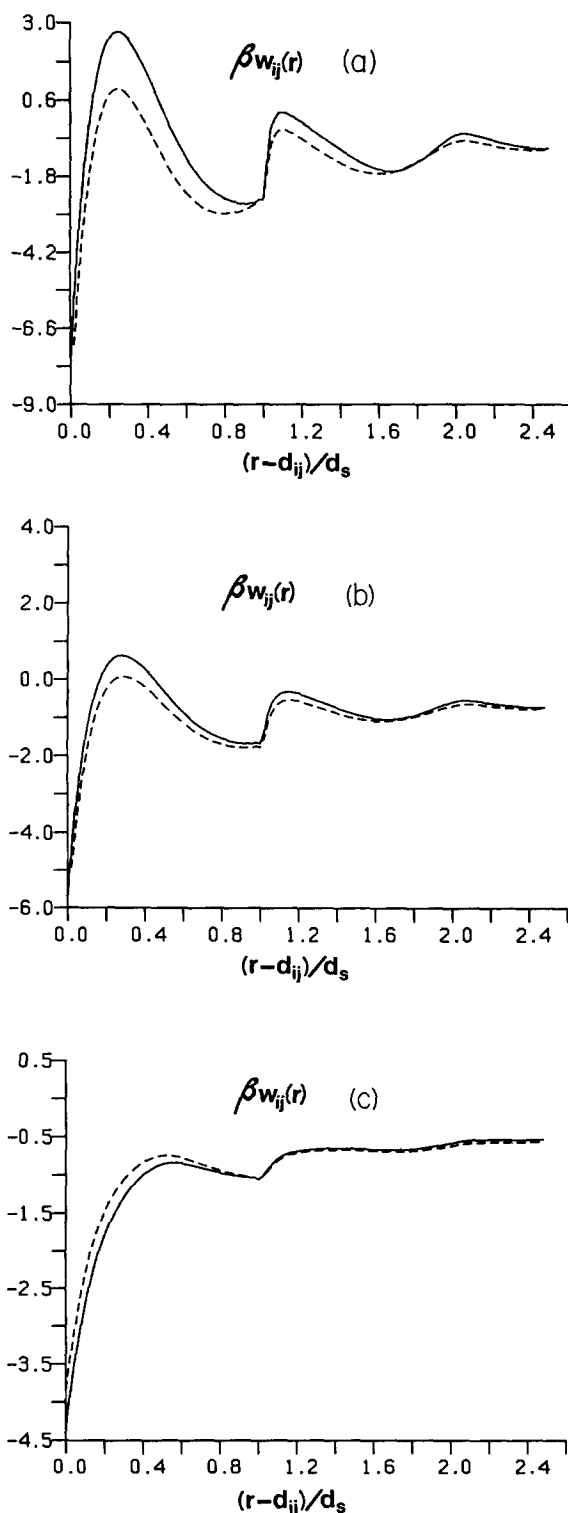

FIG. 3. Ion–ion potentials of mean force for: (a) Li⁺/F⁻, (b) Na⁺/Cl⁻, and (c) M⁺/Br⁻. The solid and dashed curves are for models I and III, respectively.

model I at short range. This inversion of behavior is likely due to the fact that for M⁺/Br⁻ the anion is the smaller species, whereas the opposite is true for Li⁺/F⁻ and Na⁺/ Cl⁻. Since the ion–octupole interaction is relatively short ranged we would expect changes in the solvation of the
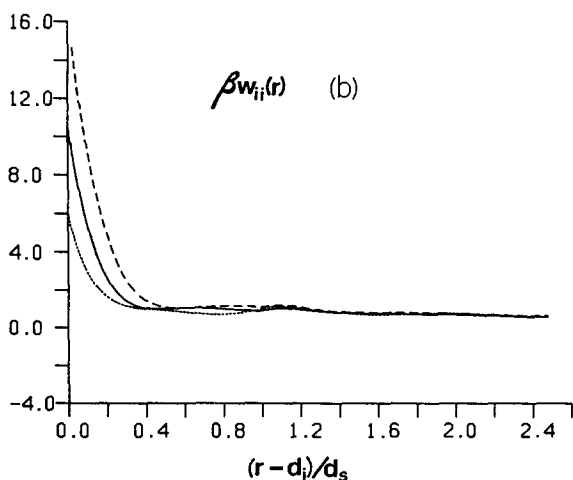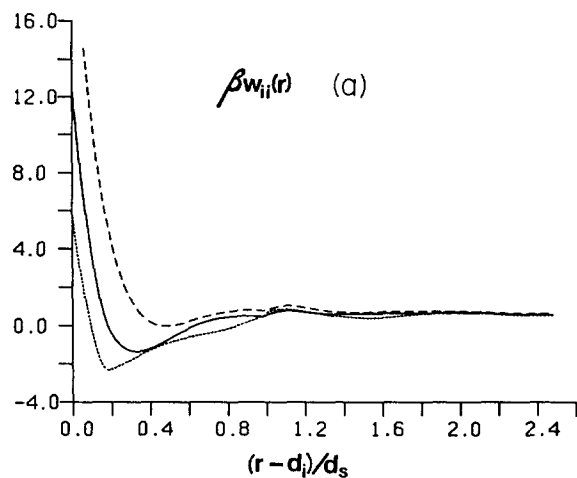
FIG. 4. Ion–ion potentials of mean force for: (a) Na^+/Na^+ and F^-/F^- and (b) Eq^+/Eq^+ and Eq^-/Eq^-. The solid curves represent the results for both the $(++)$ and $(--)$ pairs in model I. The dashed and dotted curves are for the $(++)$ and $(--)$ pairs, respectively, in model III.

FIG. 5. Ion–ion potentials of mean force for: (a) Li^+/Li^+ and (b) M^+/M^+. The solid and dashed curves are for models I and III, respectively.

smaller ion to have a greater influence upon $\beta w_{ij}(r)$.

The potentials of mean force for pairs of like ions can be dramatically altered by the presence of the octupole moment in the solvent molecule. Results for Na^+/Na^+ and F^-/F^-, and for Eq^+/Eq^+ and Eq^-/Eq^- are shown in Figs. 4(a) and 4(b), respectively. We recall again that for these pairs of equal size ions $w_{++}(r) = w_{--}(r)$ in model I. It can be seen from Fig. 4 that in solvent III this symmetry is broken in a rather striking fashion. In both cases the contact value for the negative pair is greatly reduced and the value for the positive pair is increased by roughly an equivalent amount. For the smaller ions [cf. Fig. 4(a)] the minimum at short range is significantly reduced in depth for Na^+/Na^+ but increased for F^-/F^-. Thus, the bridging structures thought[23] to give rise to these short range minima are stabilized by the octupole moment for negative ions and destabilized for the positive case. We note that the model III results are qualitatively consistent with those found[23,24] for ions immersed in other water-like solvents.

The potentials of mean force for Li^+/Li^+ and M^+/M^+ are shown in Figs. 5(a) and 5(b), respectively. It can be seen
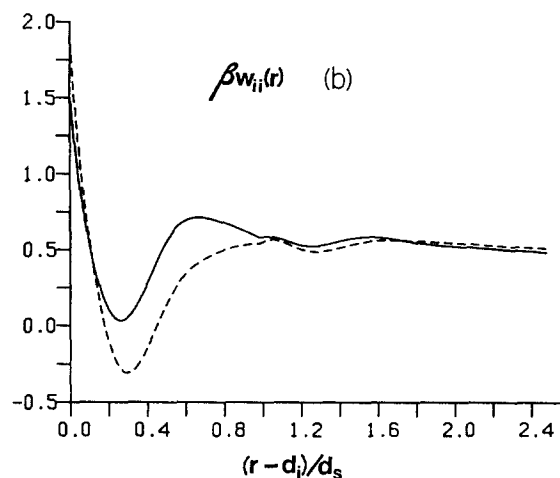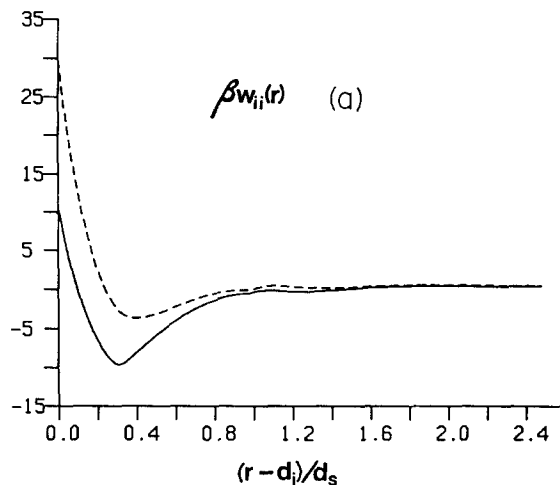
that for the small Li^+ ions the influence of the octupole is very large leading to a greatly increased average repulsion at contact. Also, the minimum at short range is reduced in depth from roughly $-10kT$ to $-4kT$. For the large M^+ ions the octupole induced effects differ in some respects from the smaller ion case. The repulsion at contact still increases, but the short-range minimum is now increased rather than decreased in depth. This different behavior probably reflects the fact that for pairs of large ions the short-range minimum in $\beta w_{ii}(r)$ is due to hydrophobic effects rather then resulting from solvent bridging structures. The fact that significant short-range minima are not found for ions of intermediate size such as Eq^+ and Eq^- [cf. Fig. 4(b)] supports this conclusion.

III. SUMMARY AND CONCLUSIONS

This paper describes a theoretical study of a variety of univalent ions immersed in different water-like solvents. Electrostatically model I is characterized by dipole and tetrahedral–quadrupole moments, and in this solvent positive and negative ions of equal size are solvated symmetrically. Model II includes the true quadrupole tensor and the solva-

tion symmetry is weakly broken, but the properties of solution do not differ significantly from those obtained with model I. In model III the octupole moment of the water molecule is taken into account, and it is found that in this solvent asymmetric solvation is important and can strongly influence certain thermodynamic and structural properties.

The inclusion of the octupolar interactions in model III leads to preferential solvation of anions and this effect is evident in the average ion-solvent energies and in the ion-solvent pair correlation functions. For example, is we consider Na^+ and F^- (which are of equal size in our model) the average ion-solvent energy is $\sim 20\%$ more negative for F^- than for Na^+. Furthermore, the value of the ion-solvent radial distribution function at contact is nearly twice as large for F^-, and the anion also has a significantly larger coordination number. Similar but somewhat smaller effects are observed for larger ions.

A detailed discussion is given of the partial molar volume of individual ions and it is argued that at infinite dilution at least two reasonable theoretical definitions of this quantity are possible. One definition inherently applies to neutral system [even if only one (+ −) pair is present] and leads to an expression which we call $\bar{V}_i^{0*}$. We suggest that the values obtained experimentally using ultrasonic vibration potentials or other methods actually correspond to the quantities $\bar{V}_i^{0*}$. It is shown that the physical interpretation of $\bar{V}_i^{0*}$ in terms of the ion-solvent interactions has a hidden pitfall in that the $\bar{V}_i^{0*}$ values do not in general reflect the true microscopic ion-solvent structure. Again taking the Na^+/F^- pair as an example, we find (in solvent model III) that $\bar{V}_i^{0*}$ is more negative for Na^+ than for F^- and hence one would infer that the electrostriction of the "neighboring" solvent is larger for Na^+ than for F^-. In turn this would imply that the average ion-solvent interactions are stronger for Na^+ than for F^-. However, the ion-solvent radial distribution functions and average energies clearly indicate that in fact the opposite is true. Thus we conclude that accurate information about the nature of specific ion-solvent interactions cannot be deduced from the $\bar{V}_i^{0*}$ results. We believe that this is also true of the experimental values.

This seemingly peculiar state of affairs can be understood if we consider the partial molecular volume $\bar{V}_i^0$ defined to be the volume change when a *single* ion is immersed in an infinite solvent bath. It is shown that $\bar{V}_i^0$ can differ from $\bar{V}_i^{0*}$ by a term (i.e., T_{is}^0) which depends upon coupling between ion-solvent and solvent-solvent orientational correlations. This term depends upon the symmetry of the solvent molecules and is not present for purely dipolar particles or for model I. However, such terms do occur for molecules of C_{2v} symmetry and for model III these terms make a very large contribution to $\bar{V}_i^0$ bringing the values obtained completely into line with the ion-solvent structure and interaction energies. Thus in a sense the contradictions one arrives at with $\bar{V}_i^{0*}$ arise from a mismatch between the physical picture one has of a single ion plus solvent, and the fact that these quantities are defined in an electrostatically neutral environment. The surprising result is that at least for our water-like model $\bar{V}_i^{0*}$ and $\bar{V}_i^0$ are very different indeed. It is important to emphasize, however, that both $\bar{V}_i^{0*}$ and $\bar{V}_i^0$ lead to identical

theoretical expressions for the partial molar volume of the salt since the T_{+s}^0 and T_{-s}^0 terms always cancel exactly for the charge neutral case.

Another interesting result of the present calculations is the observation that the ion-ion potentials of mean force at infinite dilution can be strongly influenced by the presence of the octupolar interactions. The effects are greatest for pairs of relatively small-like ions and generally tend to increase the ion-ion repulsion for cations and to reduce it for anions. For example, for Na^+/Na^+ and F^-/F^- the contact values $\beta w_{ii}(d_i)$ (which are equal in model I) differ by a factor of ~ 4 in model III. It is also found that the attractive well which occurs[1] for small-like ions is greatly reduced in depth for cations and is increased for anions. These observations are consistent with the results obtained[23,24] in other water-like models which solvate positive and negative ions asymmetrically.

Finally, we remark that this comparative study has demonstrated that the properties of electrolyte solutions at infinite dilution are much more sensitive to the details of the solvent model than one might have anticipated. Systematic studies of other models aimed at gaining a better understanding of this sensitivity both at infinite dilution and at finite concentrations are currently underway.

ACKNOWLEDGMENTS

[1] P. G. Kusalik and G. N. Patey, J. Chem. Phys. 88, 7715 (1988).
[2] S. L. Carnie and G. N. Patey, Mol. Phys. 47, 1129 (1982).
[3] D. Neumann and J. W. Moskowitz, J. Chem. Phys. 49, 2056 (1968). Note that more recent calculations [for example, C. Huiszoon, Mol. Phys. 58, 865 (1986); I. G. John, G. B. Bacskay, and N. S. Hush, Chem. Phys. 51, 49 (1980)] give similar results for the elements of the octupole tensor of the water molecule.
[4] P. G. Kusalik and G. N. Patey, Mol. Phys. (in press).
[5] B. E. Conway, in Physical Chemistry: An Advanced Treatise, edited by H. Eyring, D. Henderson, and W. Yost (Academic, New York, 1970), Vol. IX A.
[6] F. Garisto, P. G., Kusalik, and G. N. Patey, J. Chem. Phys. 79, 6294 (1983).
[7] D. G. Bounds, Mol. Phys., 54, 1335 (1985).
[8] J. Chandrasekhar, D. G. Spellmeyer, and W. L. Jorgensen, J. Am. Chem. Soc. 106, 903 (1984).
[9] M. Mezei and D. L. Beveridge, J. Chem. Phys. 74, 6902 (1981).
[10] R. W. Impey, P. A. Madden, and I. R. McDonald, J. Chem. Phys. 87, 5071 (1983).
[11] K. Heinzinger, Pure Appl. Chem. 57, 1031 (1985).
[12] B. E. Conway, Ionic Hydration in Chemistry and Biophysics (Elsevier, Amsterdam, 1981).
[13] P. G. Kusalik and G. N. Patey, J. Chem. Phys. 86, 5110 (1987).
[14] F. J. Millero, Chem. Rev. 71, 147 (1971).
[15] R. F. Zana and E. Yeager, J. Phys. Chem. 71, 521 (1967).
[16] P. Debye, J. Chem. Phys. 1, 13 (1933).
[17] J. G. Kirkwood and F. P. Buff, J. Chem. Phys. 19, 774 (1951).
[18] L. Blum and A. J. Torruella, J. Chem. Phys. 56, 303 (1971); L. Blum, ibid. 57, 1862 (1972); 58, 3295 (1973).
[19] P. H. Fries and G. N. Patey, J. Chem. Phys. 82, 429 (1985).
[20] D. Y. C. Chan, D. J. Mitchell, B. W. Ninham, and B. A. Pailthorpe, J. Chem. Phys. 69, 691 (1978).
[21] D. Levesque, J. J. Weis, and G. N. Patey, J. Chem. Phys. 72, 1887 (1980).
[22] G. Stell, G. N. Patey, and J. S. Høye, Adv. Chem. Phys. 38, 183 (1981), and references therein.
[23] X. Dang and B. M. Pettitt, J. Chem. Phys. 86, 6560 (1987).
[24] B. M. Pettitt and P. J. Rossky, J. Chem. Phys. 84, 5836 (1986).